SURFACE TENSION DRIVEN CONVECTION EXPERIMENT (STDCE)

S. Ostrach* and Y. Kamotani* and A. Pline+

*Department of Mechanical and Aerospace Engineering, Case Western Reserve University, Cleveland, Ohio.
+NASA Lewis Research Center, Cleveland, Ohio.

ABSTRACT

Results are reported of the Surface Tension Driven Convection Experiment (STDCE) aboard the USML-1 Spacelab which was launched on June 25, 1992. In the experiment 10 cSt silicone oil was placed in an open circular container which was 10 cm wide by 5 cm deep. The fluid was heated either by a cylindrical heater (1.11 cm dia.) located along the container centerline or by a CO_2 laser beam to induce thermocapillary flow. The flow field was studied by flow visualization. Several thermistor probes were placed in the fluid to measure the temperature distribution. The temperature distribution along the liquid free surface was measured by an infrared imager. Tests were conducted over a range of heating powers, laser beam diameters, and free surface shapes. In conjunction with the experiments an extensive numerical modeling of the flow was conducted. In this paper some results of the velocity and temperature measurements with flat and curved free surfaces are presented and they are shown to agree well with the numerical predictions.

INTRODUCTION

Surface tension variations along a liquid free surface caused by non-uniform temperature distributions induce so-called thermocapillary flows in the bulk liquid. In a terrestrial environment such flows are usually overshadowed by buoyancy-driven flows, except in configurations of small dimension (less than several mm). In the reduced gravity environment of space, however, buoyancy is greatly reduced and thermocapillarity becomes an important driving force for fluid motion (Ostrach, 1982). In such applications as crystal growth from melts, two-phase flows with heat transfer, and thermocapillary migration of bubbles and droplets, thermocapillary flow is known to play an important role. For that reason much attention has been given in recent years to thermocapillary flow analysis. Much of past work was done numerically. Since thermocapillary flow experiments in one-g must be conducted in very small systems to minimize buoyancy effects, they can cover only limited ranges of parameters.

Therefore, it is necessary to perform experiments in microgravity over a wide range of conditions to investigate and describe thermocapillary flows fully and to validate numerical analyses.

It is also known that thermocapillary flows become oscillatory under certain conditions but its cause is not yet completely understood. The least understood part is the role free surface deformability plays in the oscillation mechanism. Based on our past ground-based experimental work we suggested a physical model which emphasized the importance of deformable free surface and proposed a surface deformation parameter to represent its role in the oscillation mechanism (Kamotani et al., 1984). On the other hand, some investigators consider the oscillation phenomenon to be the result of instability that could occur even with an undeformable free surface (reviewed in Davis, 1987). According to the latter concept, only one dimensionless parameter, called Marangoni number (Ma), specifies the critical condition for the onset of oscillations. Therefore, we sought to obtain further evidence to determine the importance of free-surface deformation by conducting experiments in space over a wide range of conditions.

For those reasons we conceived a series of experiments to study thermocapillary flows in microgravity. The first experiment, called the Surface Tension Driven Convection Experiment (STDCE), was conducted on the first U.S. Microgravity Laboratory Mission (USML-1) on the Space Shuttle Columbia (STS-50) which was launched on June 25, 1992. The main objectives of the STDCE were to study the velocity and temperature fields in detail in non-oscillatory thermocapillary flows and to determine if Ma alone can specify the onset of oscillations. In a second series of experiments (STDCE-2), which is scheduled to be conducted aboard USML-2 in 1995, we will focus on the oscillation phenomenon including the measurement of free surface deformation.

In order to complement the space experiments, as well as to help design them, an extensive numerical analysis of thermocapillary flow was conducted for both flat and curved free surfaces and under steady and transient (non-oscillatory) conditions. In this paper some results of the velocity and temperature measurements with flat free surfaces are presented and compared with the numerical results. It was also found that despite the fact that Ma in the STDCE was as large as 5 times that of the critical Ma determined in one-g tests, no oscillations occurred.

I. DESCRIPTION OF STDCE

The specific objectives of the STDCE were to determine the extent and nature of thermocapillary flows, the effect of heating mode and level, the effect of the liquid free-surface shape, and the onset conditions for oscillatory flows. The detailed requirements of the experiment are given by Ostrach and Kamotani (1987). Its design and important considerations behind it are discussed by Kamotani and Ostrach (1987). The development of the STDCE flight hardware is described by Pline et al. (1990).

A. Experimental System

The basic experimental configurations are illustrated in Figs. 1 and 2. 10 cSt silicone oil was used as the test fluid in a circular container, 10 cm in diameter and 5 cm in depth. The container side was made of 5 mm thick copper with copper tubing coiled around the outside of the side wall for cooling water circulation. The top rim of the side wall had a sharp edge to pin the fluid. The bottom wall was made of plexiglass of uneven thickness (average thickness 8 mm) because of a filling hole and the attachment of lens assembly for flow visualization through the bottom wall. In order to minimize the contamination of the test fluid the container inner surface was kept clean and dry until the experiment and the fluid and the air above it were both contained within the fluid loop. Two heating modes were employed: CO_2 laser heating (called the Constant Flux Experiment (CF)) and heating by a cylindrical heater placed along the container centerline (called the Constant Temperature Experiment (CT)). The diameter of the submerged heater was set at 1.11 cm but the laser beam diameter was variable. The laser power was adjustable from 0.2 to 3 watts and the submerged heater power from 1 to 20 watts. The mean absorption length of CO_2 laser (10.6 μm wavelength) by the test fluid was measured to be 0.060 mm (Pline et al., 1990), so the laser beam was absorbed within a relatively very short distance from the free surface. The emissivity of the fluid surface was determined to be 0.9 (Pline et al., 1990). The free surface shape was varied by adjusting the total volume of fluid in the container. Fig. 2 shows flat and curved surfaces for the baseline tests but in the actual experiment additional tests with other curved surfaces, including a convex shape in the CF configuration, were conducted. Fig. 3 shows those surface shapes. Each shape was set within 1 mm of the prescribed location. The temperature field in the bulk fluid was studied by thermistors. Nine probes were used to measure temperature at various locations in the fluid and in the container walls. Their positions are shown in Fig. 4. The top of the thermistor No. 1 touched the free surface. In addition, one probe measured the ambient temperature above the fluid free surface and thermistors monitored the submerged heater shell temperature. The three probes along the container centerline were removed during the CT tests. The diameter of the thermistors in the fluid was 0.5 mm. The temperature data were taken once every 100 milliseconds during tests, digitized, and stored. They were downlinked during certain times to the ground station where we monitored the experiment. The resolution of the digital data was 0.1 °C and the accuracy of thermistor sensors was 0.1 °C.

To obtain information on the temperature distribution along the free surface, which is important because it is directly related to the driving thermocapillary force, a thermographic technique was employed. The infrared imaging system used in the STDCE is described by Pline and Butcher (1990). The operating wavelength was 8-14 μm and the mean absorption length of the fluid in that range was

measured to be 0.012 mm. As will be discussed later, the thermal boundary layer thickness along the free surface can become comparable to the above absorption length in certain relatively small areas but along most of the free surface the boundary layer is much thicker than the absorption length, so the infrared data represents the surface temperature well. The minimum detectable temperature difference was 0.1°C and the spatial resolution was 1 mm. Its feasibility and accuracy were checked in the ground-based experiment (Pline, 1988). This technique was also found to be very useful in studying the oscillation phenomenon (Kamotani et al., 1992).

The flow field was studied by flow visualization. Fifty micron alumina particles were used as tracers. They were illuminated by a 1 mm thick laser light sheet to study the flow in one cross-sectional plane of the container. Since the container side wall was made of copper to obtain a uniform wall temperature, a CCD camera was attached to the transparent bottom wall (see Fig. 1) for recording. Because of the bottom viewing the video image of the illuminated cross-section was distorted (keystone effect). The video record of the flow is being analyzed using a particle image velocimetry (PIV) technique. The technique is explained by Wernet and Pline (1991). The keystone effect is corrected in the analysis.

The hardware for the STDCE is discussed in more detail by Pline, et al. (1993).

B. Parametric Ranges

The important dimensionless parameters for the present experiment in the case of flat free surface are: Ma (Marangoni number) $=\sigma_T \Delta T H/\mu\alpha$, Pr (Prandtl number) $=\nu/\alpha$, Ar (aspect ratio) = H/R, Hr (relative heater size) = D_H /D, where σ_T is the temperature coefficient of surface tension, ΔT the net temperature variation along free surface, H the fluid depth, D the container diameter, R the radius, D_H the heating zone diameter, ν the kinematic viscosity of the fluid, μ the dynamic viscosity, and α the thermal diffusivity. In the CT configuration ΔT is the temperature difference between the heater and the side wall. Since total heat input is specified in the CF tests, the ΔT is not known a priori. However, because the thermocapillary flow driving force is closely related to ΔT and to make comparisons between the CT and CF tests convenient, a Ma based on ΔT is used in both cases in the present paper, ΔT being determined from the numerical analysis for the CF tests.

In one-g heat loss occurs at the free surface mainly through natural convection in the surrounding air but in microgravity radiation loss to the enclosure wall becomes important. Since the temperature difference between the free surface and the surroundings is relatively small compared to their absolute temperatures, the radiation loss can be represented by Ra(radiation parameter) = $\epsilon\sigma Ta^3H/k$, where ϵ is the emissivity of the fluid free surface, σ the Stefan-Bolzmann constant, Ta the temperature of the surroundings, and k the thermal conductivity of the fluid.

The range of each parameter covered in the STDCE was as follows: $3.6 \times 10^4 \leq Ma \leq 3.1 \times 10^5$, $78 \leq Pr \leq 97$, Ar = 1.0, Hr = 0.11 for CT and 0.05, 0.1, and 0.3 for CF, and Ra = 0.5. The physical properties are evaluated at the mean fluid temperature in the container. The range of Pr reflects the fact that the fluid viscosity varies with temperature. In our ground-based tests in the CT configuration using a small container (4 mm dia.), the critical Ma for the onset of oscillations was found to be 6.5×10^4 (Kamotani et al., 1992), so the maximum value of Ma in the STDCE was about 5 times of that. As discussed in the Introduction, we found that the deformability of the free surface is important in the oscillation mechanism and proposed the surface deformation parameter S, which is defined as $S = \sigma_T \Delta T/\sigma(1/Pr)$, to represent it, when Pr is larger than unity (Kamotani et al., 1984). The critical value of S determined in our one-g tests was 9×10^{-3} for Ar = 1 (Kamotani et al., 1992) but in the STDCE the maximum value of S was 2.5×10^{-3}, so based on our concept the flow in the STDCE should not oscillate.

II. NUMERICAL ANALYSIS

The program for flat free surface is based on the SIMPLER algorithm by Patankar (1980). The flow is assumed to be laminar, incompressible, and axisymmetric. The fluid properties are considered to be constant except for viscosity which varies with temperature. The program analyzes both transient and steady states. It turns out that all the temperature data taken in the STDCE were in transient state although we had planned to obtain some steady state data.

In the CT configuration the measured temperatures of heater and side wall are used as inputs. Both temperatures changed with time during the tests. In the CF case the measured values of laser power and side wall temperature, and the beam diameter are the inputs. The emissivity and the absorption length are also taken into account. The coordinate system used in the analysis is defined in Fig. 4. The velocity components (u, v) and stream function ψ are made dimensionless by $\sigma_T \Delta T/\mu$ and $\sigma_T \Delta T R H/\mu$, respectively. The temperature T is non-dimensionalized as $\theta = (T - Tc)/\Delta T$, where Tc is the side wall temperature.

A non-uniform grid system is adopted with meshes graded toward the hot and cold walls and toward the free surface. In the CT cases due to the presence of a thin thermal boundary layer along the heater surface the free surface temperature varies very sharply near the heater. As a result the free surface velocity increases very sharply in that region and an accurate resolution of the surface velocity distribution near the heater is the most important requirement for the numerical grid. In Fig. 5a the surface velocity distributions computed with three different grids are shown. The computed case corresponds to the main CT test and is discussed in detail below. The 46 x 41 (radial x vertical) grid with the smallest radial mesh size of 0.001 next to the heater is not adequate. The 58 x 51 and 67 x 60 grids

with the smallest mesh sizes of 0.0005 and 0.0003, respectively give nearly the same distribution. With all three grids the maximum stream function and the total heat transfer rate are all within 1% of each other. Therefore the 58 x 51 grid is used both for the steady and transient CT computations. In the CF configuration there exists a very thin thermal boundary layer along the free surface in the region heated by the laser beam, so an accurate prediction of the surface temperature distribution near the heated region becomes important. In Fig. 5b the surface temperature distributions computed with three different grids, 37 x 40, 46 x 51, and 58 x 60 with the smallest axial mesh sizes next to the free surface of 0.005, 0.001, and 0.0005, respectively are shown for the main CF test. Based on Fig. 5b the 46 x 51 grid is used for the CF transient and steady analysis.

The program for curved free surfaces is explained in Kamotani and Platt (1992). The computational domain with curved free surfaces is transformed into a rectangular domain by a coordinate transformation and the velocity and temperature fields are solved by a finite-difference scheme.

III. RESULTS AND DISCUSSION

In the STDCE a total of 20 CF and 18 CT tests were conducted with flat and curved free surfaces but many of them were run only for 10 minutes to study if the flow became oscillatory. It had been estimated that it takes about one hour after the flow is started to obtain hydrodynamic as well as thermal equilibrium. Considering that relatively long transient period we had decided to conduct only one CF and one CT 1-hour test with flat free surfaces to study the complete transient flow and thermal development. Those two tests are discussed first.

A. CT One-hour Test

Before the test we made sure that the free surface was flat and no appreciable motion existed in the fluid through video downlink. Fig. 6 shows how the heater and side wall temperature varied during the one-hour period after the heating started. The power to the heater was boosted for the first 90 seconds to shorten the warm-up time of the heater. Judging from the heater temperature overshoot in Fig. 6 the power boost was slightly too large. After the boost period the heater power was fixed but the heater temperature increased gradually throughout the one-hour period. The side wall temperature variation was relatively small, about 0.6 °C increase after one hour. The readings of the two thermistors in the side wall were the same within the resolution of the data acquisition system (0.1 °C). As for the 6 thermistors in the heater shell 4 of them, which are positioned in the top 2/3 of the heater length, read within 0.2 °C of each other (the data in Fig. 6 is the average of those) but 2 thermistors near the heater bottom read about 0.5 °C below the above average probably due to the end loss. The solid lines in Fig.

6 are the inputs to the numerical analysis.

Fig. 7 shows the computed streamlines and isotherms at t(time) = 2 min. The streamline pattern shows that the whole fluid is already in motion at this time. The observed streamline pattern at the same time is shown in Fig. 8, which was obtained by superposing several video frames of the flow. The observed pattern agrees well with the computed one in Fig. 7 in terms of the overall flow structure (unicellular motion) and the location of the cell center. The overall flow pattern changes little beyond this time. In comparison, in one-g the flow in this large system is confined to a thin region near the surface because of stratification. The isotherms in Fig. 7 suggest that over most of the flow field the temperature is basically equal to the initial temperature. The liquid initial temperature was about 0.5 °C below the side wall temperature.

The development of temperature field with time is shown in Fig. 9 based on the numerical analysis. One can see that heat is transferred from the heater by convection first along the free surface and then into the interior region. The steady state profile in Fig. 9 is computed based on the thermal boundary conditions at t = 60 min., which shows that the temperature field at t = 60 min. (Fig. 9c) is not yet steady. One reason why it did not become steady by t = 60 min. (we had estimated the transient period to be about 60 min.) was because the heater temperature kept increasing as seen in Fig. 6. Fig. 9 also shows the presence of a thin thermal boundary layer along the heater. In the CT tests thermistors No. 1 - No. 3 (Fig. 4) measured the fluid temperature. The outputs from those probes are compared with the numerically predicted values in Fig. 10 and good agreement is shown. For some reason the No. 3 probe output seemed to be too high because, although it was placed below the No. 2 probe (Fig. 4), its reading was always above that of No. 2, which does not seem to be correct (see the isotherms in Fig. 9). In any case the difference between the No. 3 probe reading and the numerical prediction is at most 0.4 °C, which is only 3% of ΔT. As shown in Fig. 10b, relative to the overall temperature variation in the liquid agreement between the analysis and data can be said to be excellent (for clarity only Nos. 1 and 2 readings are shown in Fig. 10b). As mentioned above, the fluid temperature was still increasing after the one-hour period.

The infrared imager did not require in situ calibration but for a reason not yet fully understood its readings seemed to have shifted judging from a comparison of its measurement of the fluid initial temperature with that measured by the thermistors. It was calibrated before and after the flight but no drifting was found. For that reason instead of determining the absolute temperature of the free surface we computed the surface temperature increase above the initial temperature. Fig. 11 shows the relative surface temperature distributions at t = 10 and 60 min. The data and numerical prediction agree very well. As seen in Fig. 11 the surface temperature drops sharply near the heater and, as a result, the surface velocity increases very sharply and attains its peak near the heater as Fig. 5a shows. By

comparing the profiles at t = 10 and 60 min., one sees that the overall profile does not change much with time, only it shifts as the fluid warms up, which explains why the velocity field does not change much with time, the driving force being dependent on the slope of the profile.

The total heat transfer at the heater is calculated to be 1.18 W while the total power input to the heater was measured to be 1.2 W, so about 2% of the input is lost by conduction through the base of the heater. Of 1.18 W of the net heat input to the fluid 14% is lost by radiation from the free surface according to the numerical analysis. The ratio of the net heat input to the total heat out from the fluid (radiation loss plus conduction at the cold wall) is computed to be 1.19 at t= 60 min., showing again that the temperature field was not in equilibrium at that time.

The velocity vectors determined from the particle motions at t = 10 min. are presented in Fig. 12. The velocity is relatively large in the region near the top half of the heater. Although there is a very strong flow along the free surface close to the heater (see Fig. 5a), the present flow visualization did not detect it because the tracer particles did not go into that small corner region.

The measured velocity distributions are compared with the computed ones in Fig. 13. The axial velocity distribution at Z/H = 0.89 (Fig. 13a) and the radial velocity distribution at r/R = 0.23 (Fig. 13b) are shown. Those locations cover the region of large velocity in Fig. 12. At present the velocity field analysis is not yet complete and the data presented herein are still preliminary. Fig. 13 shows two sets of data, one from the right cross-section in Fig. 12 and the other from the left. In Fig. 13a the data and the prediction differ as much as 40% but the predicted general trend agrees with the data. We have to analyze much more data before we can make a definite statement about the comparison. The agreement in Fig. 13b is better except near the free surface where, as discussed above, the measurement did not show a large velocity region close to the surface.

B. CF One-hour Test

The thermal conditions for the CF test are shown in Fig. 14 . The laser beam power remained constant at 0.48 W throughout. The beam diameter was 1.0 cm. However, the side wall temperature kept increasing and changed by 1.5 °C (15% of ΔT) after one hour. Since in the above CT test the side wall temperature did not change that much despite the fact that the heat input to the fluid was greater, the side wall temperature increase in the CF test was not because of the heat input from the laser beam. Considering the fact that the air temperature above the fluid also increased by the same rate as Fig. 14 shows, the increase is considered to be due to the ambient temperature increase due probably to an increase in thermal loading of the Shuttle avionics air system. In all other tests the side wall temperature remained at about 25 °C. The solid lines in Fig. 14 are the inputs to the numerical analysis. The air temperature is assumed to represent the surrounding wall temperature in the calculation of the radiation

loss from the free surface.

Fig. 15 shows the computed and measured streamlines at t = 2 min. They agree well. The flow structure is unicellular as in the CT configuration.

The computed isotherm patterns at various times are presented in Fig. 16. The steady state pattern is based on the thermal conditions at t = 60 min. The initial liquid temperature was about 0.6 °C below the side wall temperature. At t = 10 min., heat was spread only along the free surface and most of the fluid temperature remained unheated. Even at t = 30 min., a large portion of the fluid had a temperature below the side wall but convection was beginning to heat up the interior. At t = 60 min., most of the fluid had a temperature just above the side wall temperature but the temperature distribution was not yet close to the steady profile. The main reason why the fluid temperature remained low compared to the side wall for that long time was the continuous increase of the latter temperature as discussed above. Also compared to the CT case the total heating area was smaller in the CF test, so the bulk temperature remained relatively low in the latter case.

Fig. 17a shows the computed maximum fluid temperature and comparison between the Nos. 1 and 2 thermistor readings and the numerical prediction. The maximum temperature kept increasing partly because of the side wall temperature increase and partly because the temperature field was not in equilibrium. The figure shows good agreement between the data and the prediction. In Fig. 17b the temperature scale is expanded to show three thermistor readings. As discussed in the CT case, the reading of No. 3 thermistor seemed to be slightly too high (nearly close to the reading of the probe at the free surface) but the difference between the data and the prediction is about 0.4 °C which is only 4.5% of ΔT. In the CF test the three thermistors along the container centerline gave additional data and their readings are given in Fig. 17c along with the numerical prediction. Their readings are all close and the predicted temperature variations follow the data closely. According to the isotherms in Fig. 16 the thermal boundary layer thickness along the free surface is less than 1.5 mm near the center, so the No. 5 thermistor, which was located at 2 mm from the surface, was just outside the boundary layer.

The infrared imager data are compared with the predicted relative surface temperature distributions at t = 10 and 60 min. in Fig. 18. They agree well but near the heated region the imager data was lower than the prediction because of the presence of a very thin thermal boundary layer there. Because of the thin boundary layer practically there is no accurate way to measure the surface temperature near the middle. The data at r/R = 0.5 agrees with the No. 1 thermistor data.

As for the overall thermal balance based on the numerical analysis, 14% of the total heat input to the fluid is lost by radiation from the free surface at t = 60 min. The ratio of the total heat input to the total heat out from the fluid is 3.4 at t = 60 min. so that the temperature field is still very far away from equilibrium even after one hour. The overall ΔT is 10 °C when a steady state is reached as seen in Fig.

5b but ΔT at t = 60 min., is still about 9 °C according to Fig. 17a.

The velocity vectors at t = 10 min., are given in Fig. 19 and Fig. 20 shows the measured and computed velocity distributions at selected locations. The agreement between them is better than that in the CT configuration (Fig. 13) and in this particular instance a few particles gave large velocities near the surface.

By comparing the results of the CT and CF tests presented above one can say that although the flow structures are similar (simple unicellular structure), the temperature fields are different: In the CT case the overall fluid temperature is higher and there exists a very noticeable thermal boundary layer all along the heater surface while in the CF case a thermal boundary layer exists along the free surface mainly in the heated region. In both cases the free surface temperature drops sharply in a relatively small region near the center (the so-called hot-corner region) and the flow is driven mainly in the hot-corner region. Although no oscillations were found in the present experiment, our ground-based tests have shown that the oscillation phenomenon is very much influenced by the heating mode.

C. Curved Free Surface Tests

The analysis of the data from the curved free surface tests has just begun, so not much data can be presented herein. An example of streamline pattern with a curved free surface is presented in Fig. 21 and it is compared with the numerical result. The predicted flow pattern agrees well with the data. The flow structure is still unicellular. One major objective herein is to study how the free surface shape affects the flow structure. One aspect studied so far is given in Fig. 22, where the location of the cell center is shown for various surface shapes. The predicted locations are in general agreement with the measured ones. When the free surface is flat or convex, the cell center is located around mid-radius. When the surface is concavely curved, the flow along the free surface turns around sooner because the flow passage toward the top cold wall region narrows and consequently the cell center moves toward the centerline. However, when the surface is highly concave, the fluid height near the center becomes small and consequently the fluid speed decreases rapidly when the fluid moves away from the center because of increasing flow area. Therefore, the main motion is seen only near the center, which produces one cell. The fluid speed is quite small away from the center but since the fluid volume involved in the weak motion is very large, a second cell is produced in the region (Fig. 22). The fluid rotation direction is the same in both cells. A more detailed flow analysis is in progress.

CONCLUDING REMARKS

Some of the velocity and temperature data taken in the STDCE experiment conducted aboard the USML-1 Spacelab in 1992 are presented. The results for one-hour CT (Constant Temperature) test

and also for one-hour CF (Constant Flux) test and some preliminary results for curved surface tests are given and compared with the results of the numerical analysis conducted in conjunction with the experiment. The tests covered a range of Ma up to 3.1×10^5 . Aside from some problems discussed above, the hardware performed well generally and a large amount of valuable data were collected. Much of the data are still being analyzed. The temperature data shown in the present paper agree well with the numerical predictions. A validation of a numerical analysis for thermocapillary flow in such a high Marangoni range has not been done in the past. A total of 20 CF and 18 CT tests were conducted with flat and curved free surfaces under varieties of conditions. No oscillations or instabilities were observed in any of the tests. G-jitter caused by thruster firings induced small but visible free surface disturbances but did not change the flow field appreciably.

ACKNOWLEDGMENTS

The authors wish to express their appreciation to many people, especially the NASA Lewis Research Center engineering and operations teams, who contributed to make the STDCE a successful and important experiment. Special thanks to Dr. Eugene Trinh who, as a payload specialist aboard the USML-1, conducted the STDCE tests tirelessly and expertly for many hours. We also gratefully acknowledge the financial support of NASA for this experiment. The work done at Case Western Reserve University was supported by NASA under contract NAS3-25973 with Mr. T. P. Jacobson of the NASA Lewis Research Center as the Project Manager and Dr. R. Thompson as the Project Scientist.

REFERENCES

1. Davis, S. H., 1987, *Thermocapillary Instabilities*, Annual Review of Fluid Mechanics, Vol. 19, pp. 403-435.

2. Kamotani Y., Ostrach, S., and Vargas, M., 1984, *Oscillatory Thermocapillary Convection in a Simulated Floating-Zone Configuration*, Journal of Crystal Growth, Vol. 66, pp. 83-90.

3. Kamotani, Y. and Ostrach, S., 1987, *Design of a Thermocapillary Flow Experiment in Reduced Gravity*, Journal of Thermophysics and Heat Transfer, Vol. 1, pp. 83-89.

4. Kamotani, Y. and Platt, J., 1992, *Effect of Free Surface Shape on Combined Thermocapillary and Natural Convection*, Journal of Thermophysics and Heat Transfer, Vol. 6, No. 4, pp. 721-726.

5. Kamotani, Y., Lee, J. H., and Ostrach, S., 1992, *An Experimental Study of Oscillatory thermocapillary Convection in Cylindrical Containers*, Physics of Fluids A, Vol. 4, pp. 955-962.

6. Ostrach, S., 1982, *Low-Gravity Fluid Flows*, Annual Review of Fluid Mechanics, Vol. 14, pp. 313-345.

7. Ostrach, S. and Kamotani, Y., 1989, *Science Requirements Document for the Surface Tension Driven Convection Experiment in Reduced Gravity*, Case Western Reserve University, Cleveland, Ohio.

8. Patankar, S. V., 1980, Numerical Heat Transfer and Fluid Flow, Hemisphere Pub., Washington.

9. Pline, A., 1988, *Surface Temperature Measurements for the Surface Tension Driven Convection Experiment*, NASA TM 101353.

10. Pline, A. and Butcher, R. L., 1990, *Spacelab Qualified Infrared Imager for Microgravity Science Applications*, Thermosense XII, SPIE Vol. 1313, pp. 250-258.

11. Pline, A., Jacobson, T. P., Wanhainen, J. S., and Petrarca, D. A., 1990, *Hardware Development for the Surface Tension Driven Convection Experiment*, Journal of Spacecraft and Rockets, Vol. 27, pp. 312-317.

12. Pline, A., Jacobson, T. P., Kamotani, Y., and Ostrach, S., 1993, *Surface Tension Driven Convection Experiment*, AIAA Paper 93-4312.

13. Wernet, M. and Pline, A., 1991, *Particle Image Velocimetry for the Surface Tension Driven Convection Experiment Using a Particle Displacement Tracking Technique*, NASA TM 104482.

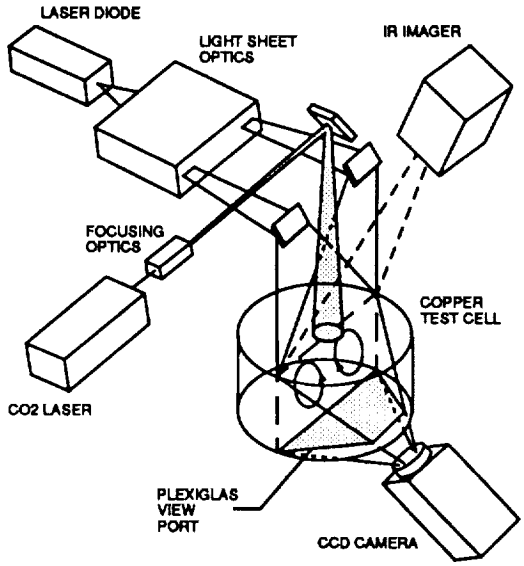

Figure 1 Experimental setup for STDCE

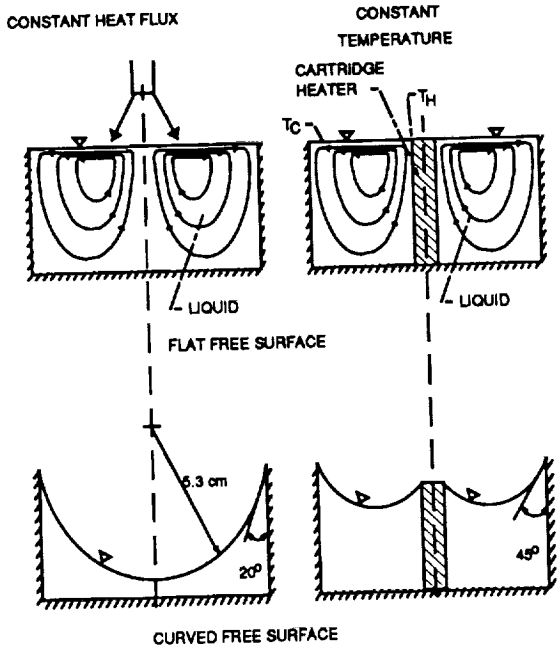

Figure 2 Basic configurations of STDCE

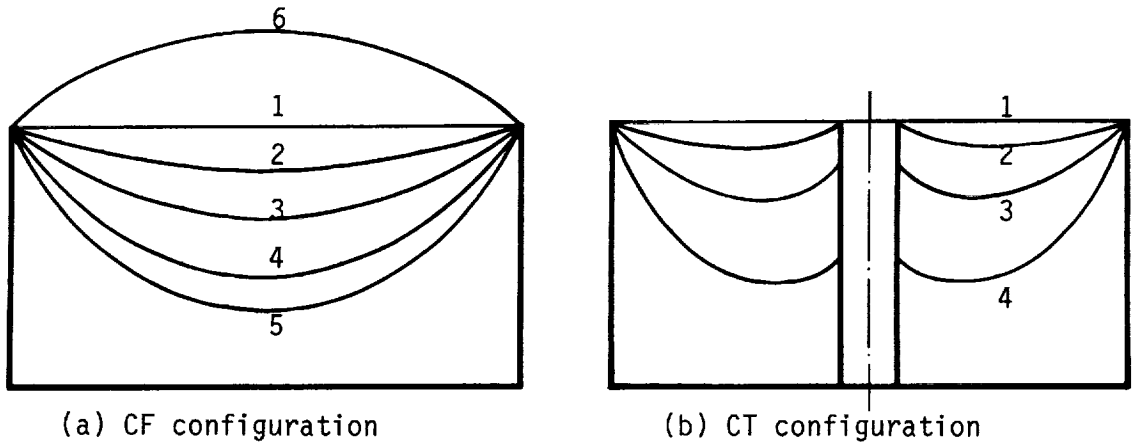

Figure 3 Free surface shapes

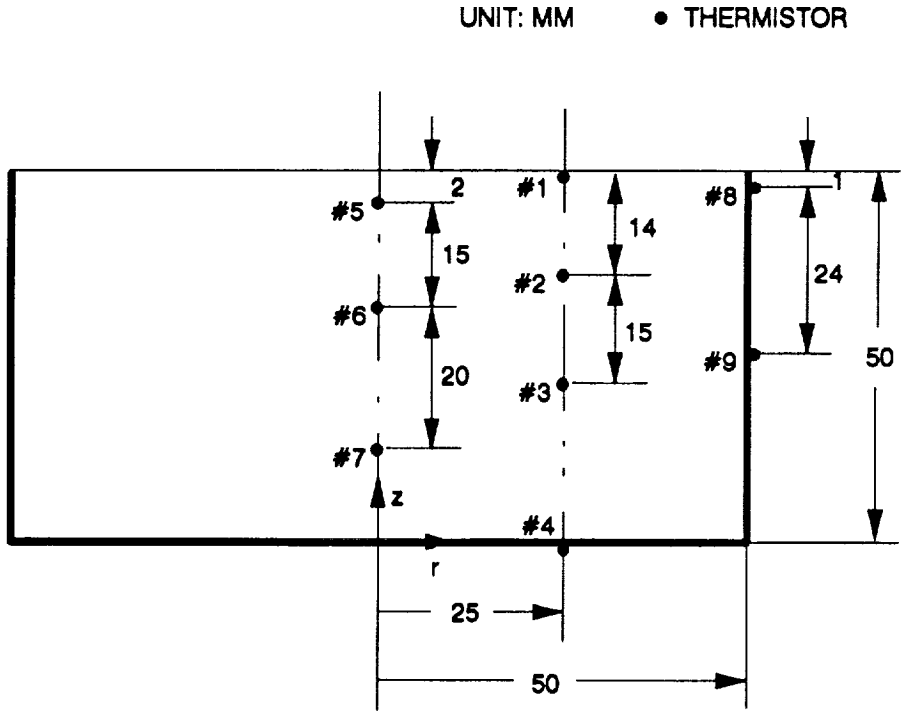

Figure 4 Location and numbering of thermistors

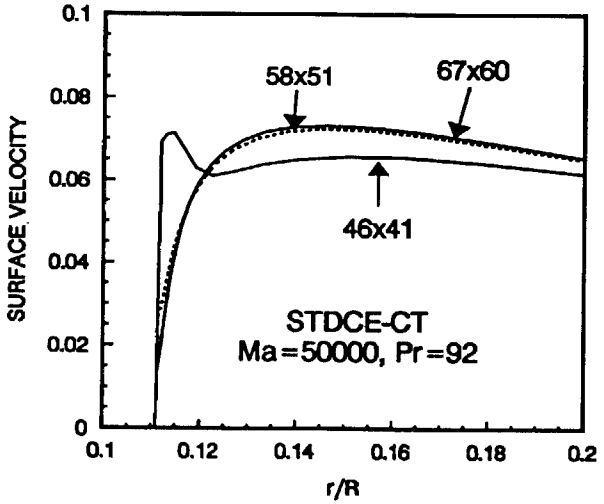

(a) Surface velocity distribution for CT test

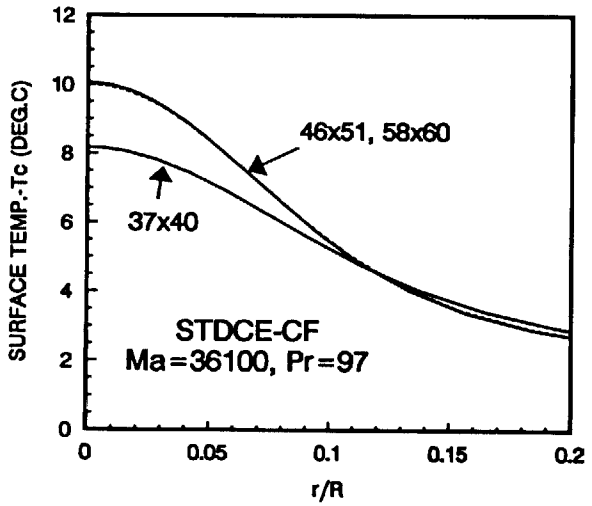

(b) Surface temperature distribution for CF test

Figure 5 Comparison of results obtained with various grid systems

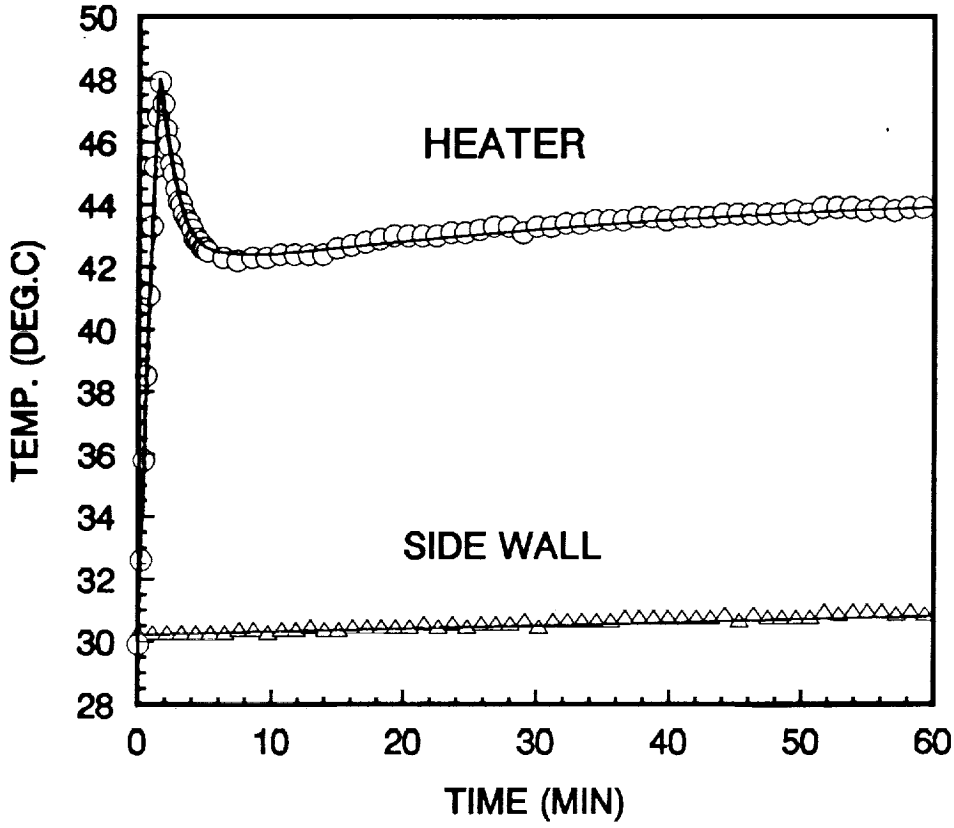

Figure 6 Variation of heater and side wall temperatures with time for CT test (symbols denote experimental data and solid lines are inputs to numerical analysis)

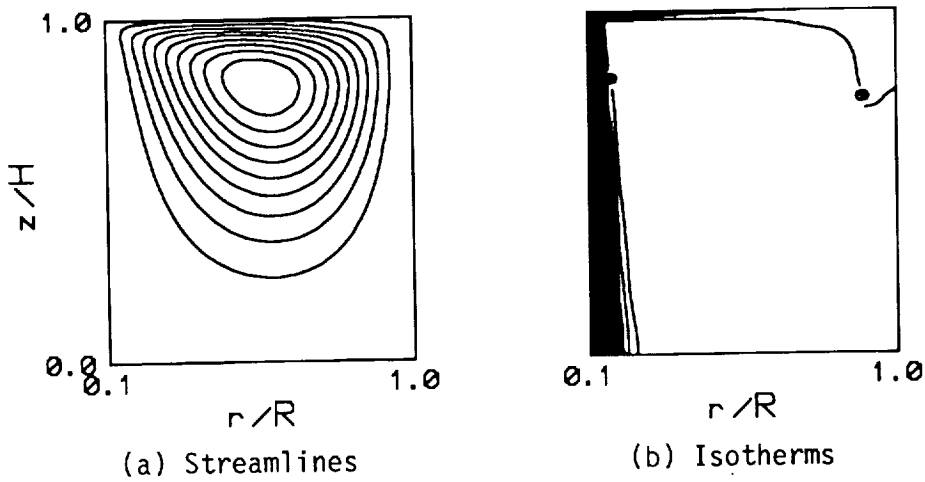

Figure 7 Streamlines and isotherms at t = 2 min. for CT test

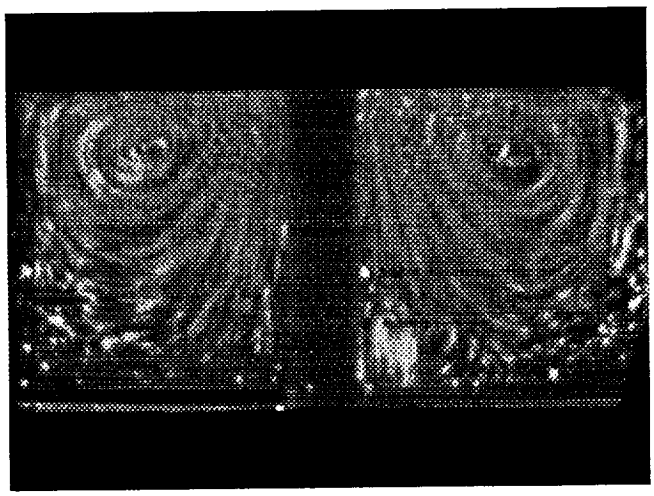

Figure 8 Observed streamlines at t = 2 min. for CT test

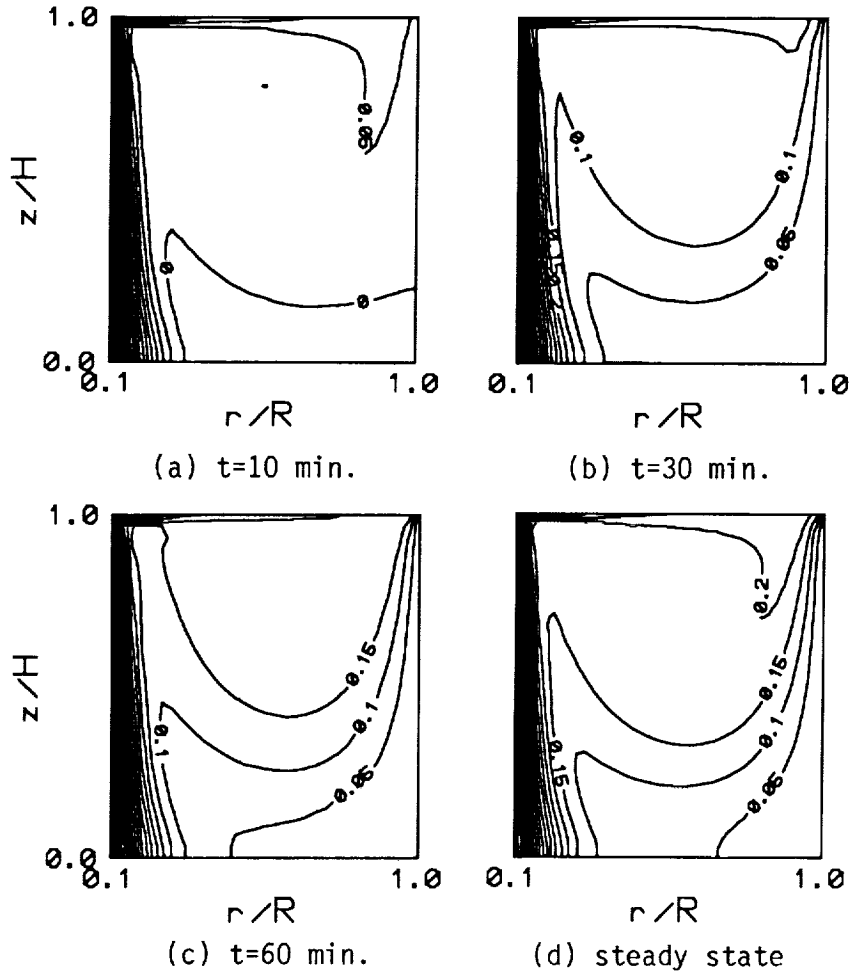

Figure 9 Isotherms at various times for CT test

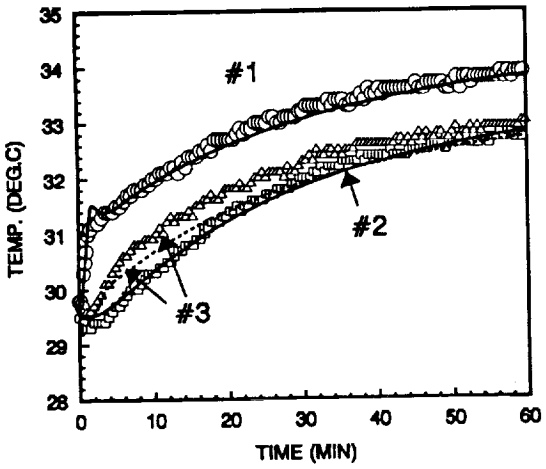

(a) Fluid temperature variation

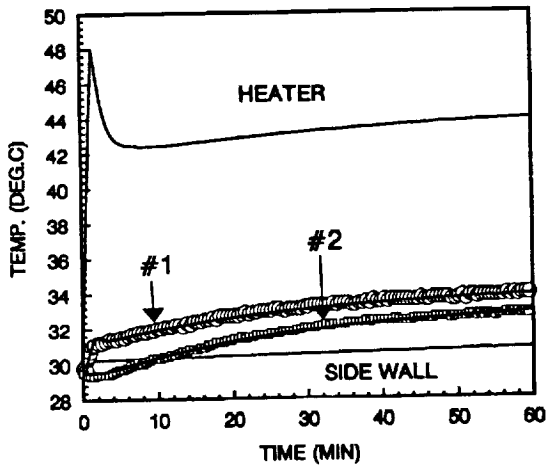

(b) Fluid temperature in comparison with boundary temperatures

Figure 10 Comparison of thermistor data with numerical result for CT test

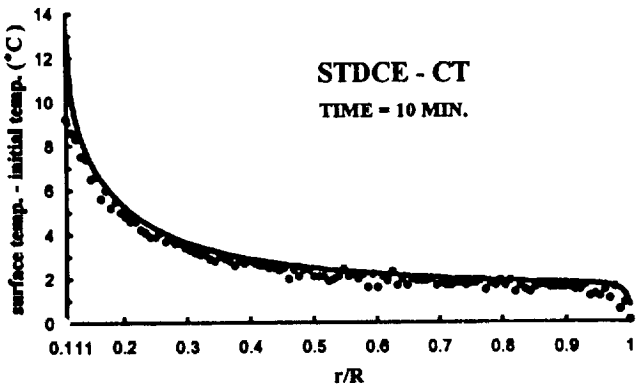

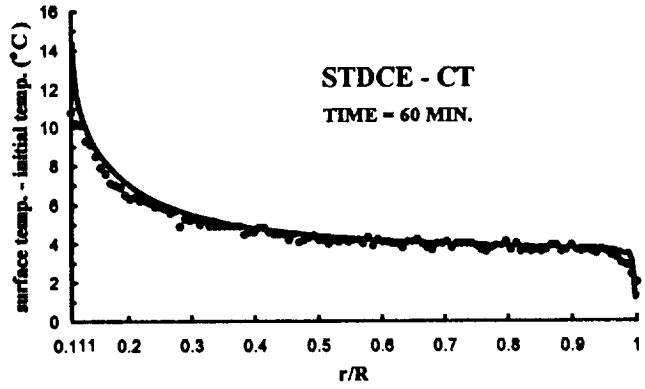

Figure 11 Comparison of infrared imager data with numerical result for CT test (points are experimental data and lines are numerical results)

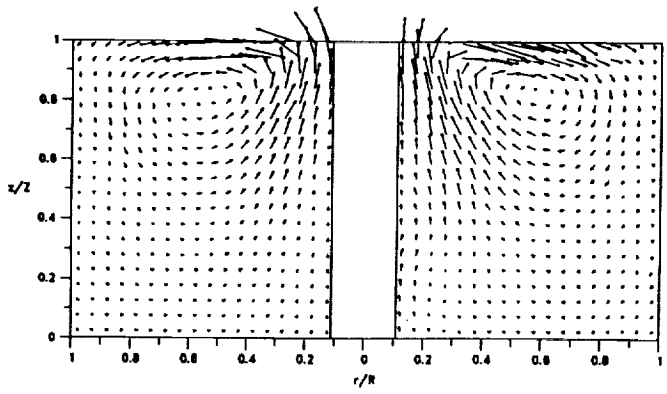

Figure 12 Measured velocity vectors at t = 10 min. for CT test

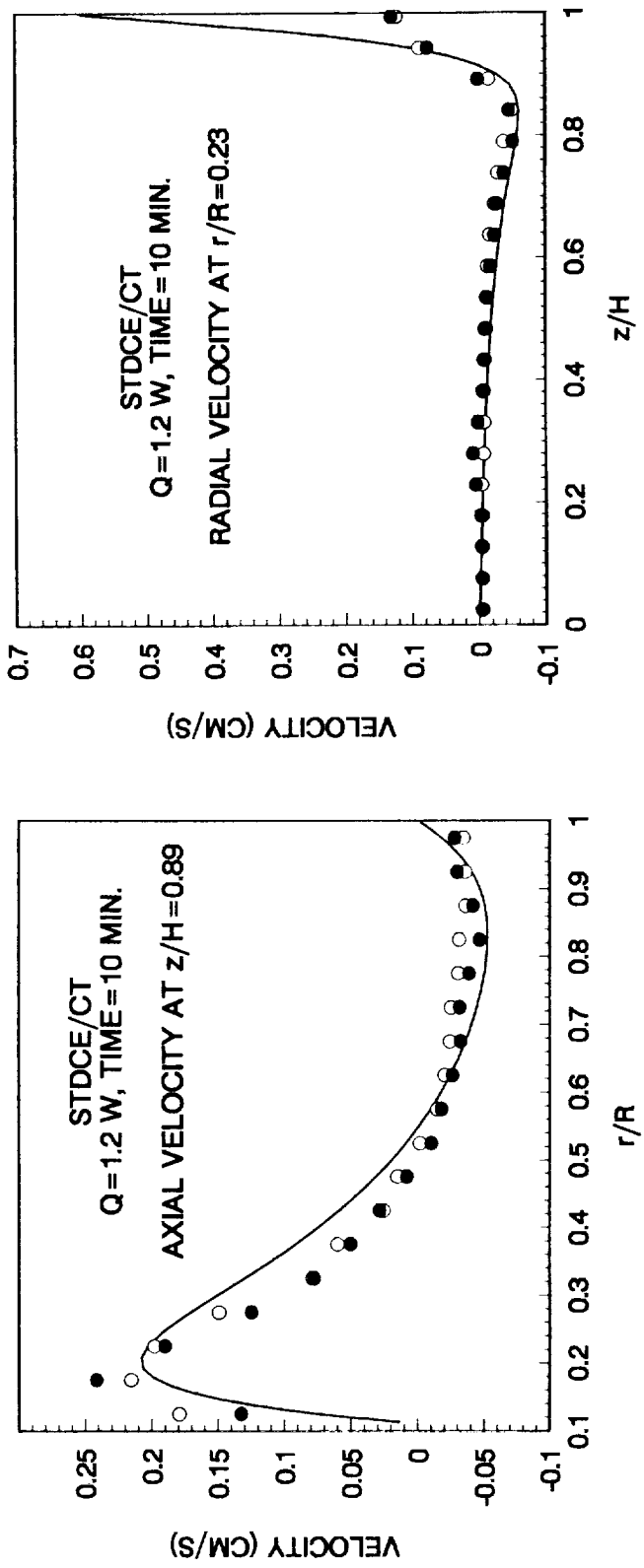

Figure 13 Measured and computed velocity distributions at t = 10 min. for CT test

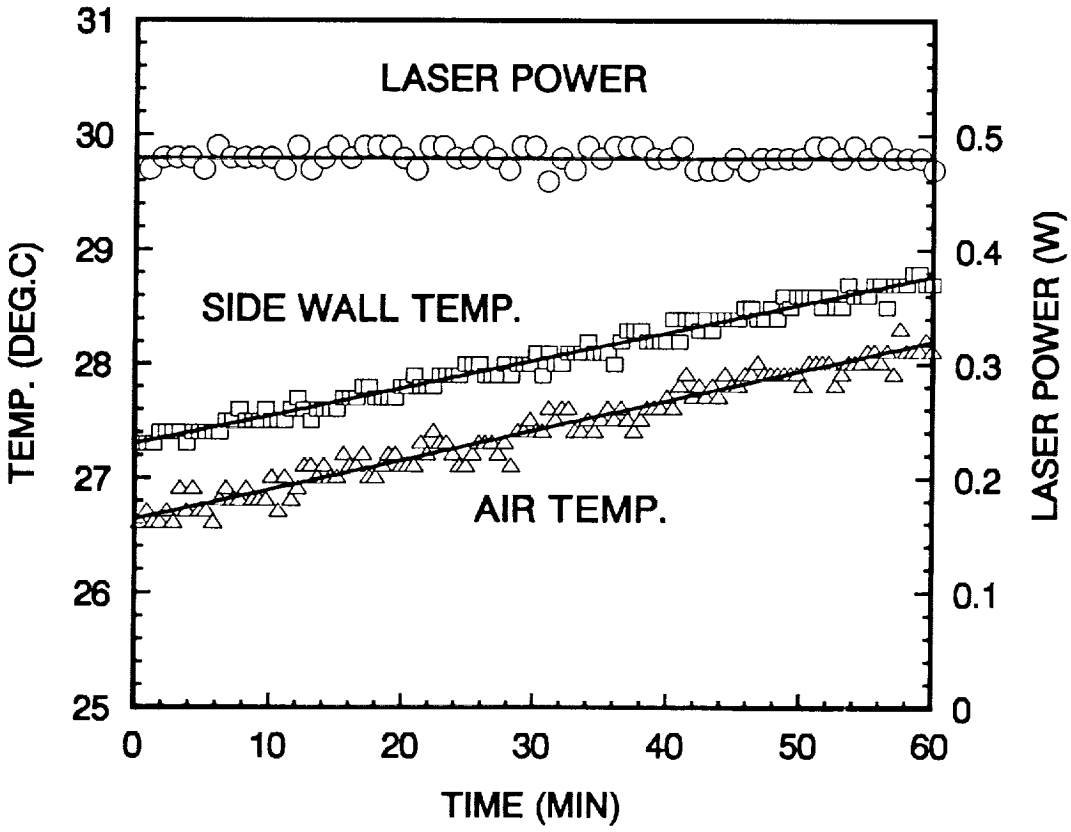

Figure 14 Thermal boundary conditions for CF test (symbols denote experimental data and solid lines are inputs to numerical analysis)

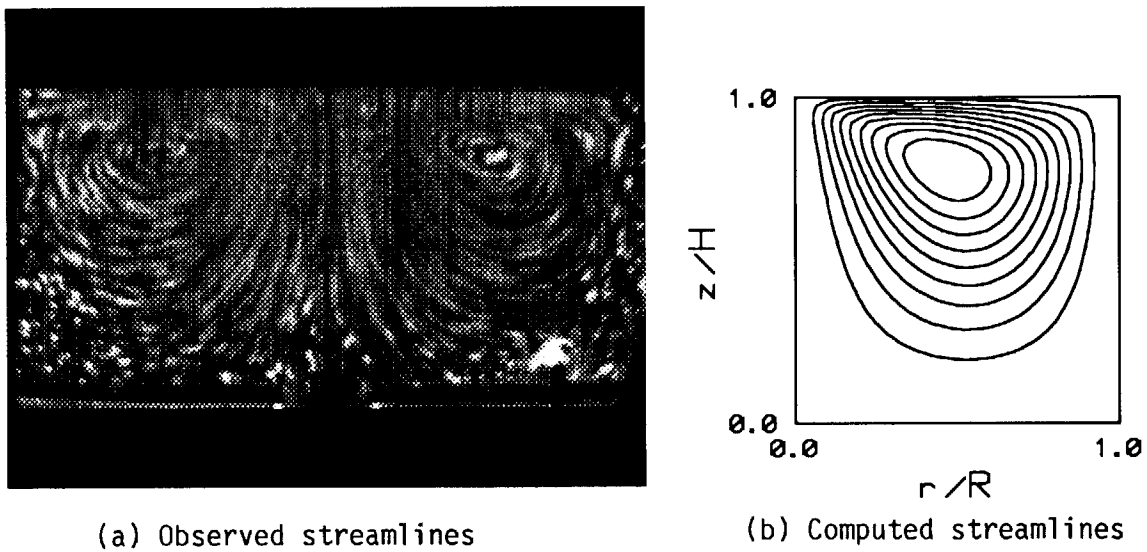

(a) Observed streamlines

(b) Computed streamlines

Figure 15 Observed and computed streamlines at t = 2 min. for CF test

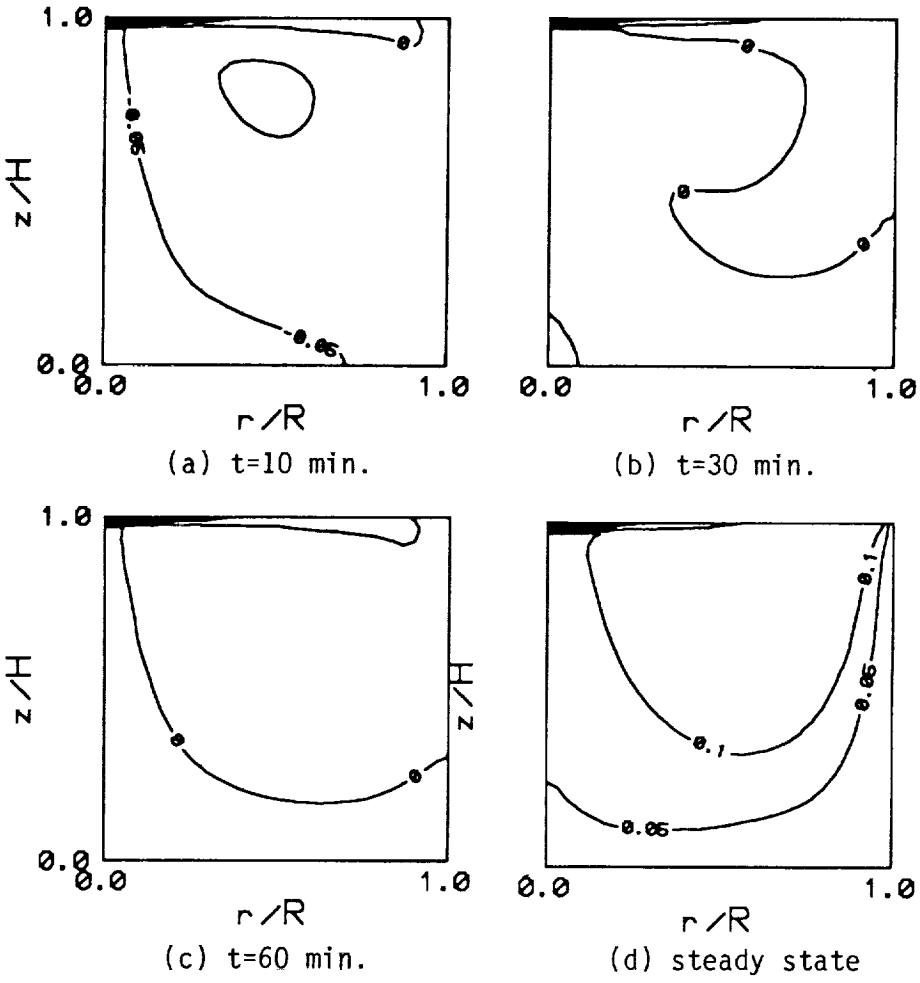

Figure 16 Isotherms at various times for CF test

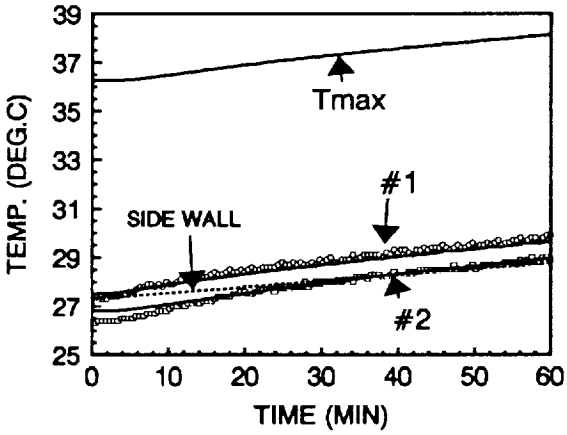

(a) Fluid temperature variation

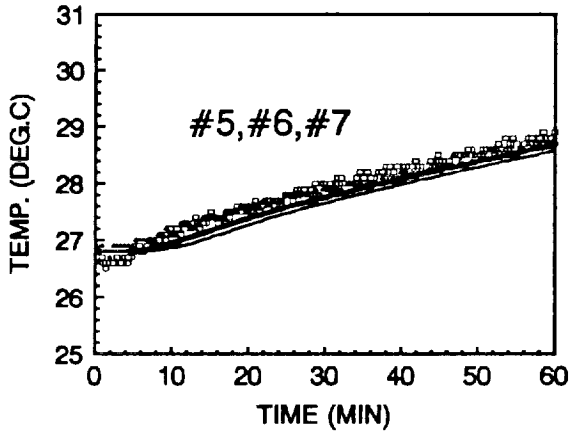

(c) Fluid temperature at r/R=0

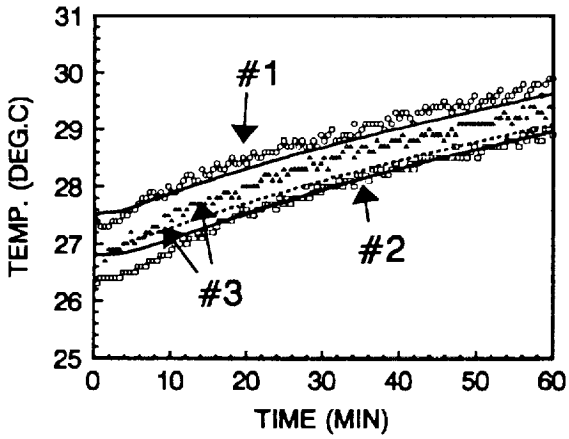

(b) Fluid temperature at r/R=0.5

Figure 17 Comparison of thermistor data with numerical result for CF test

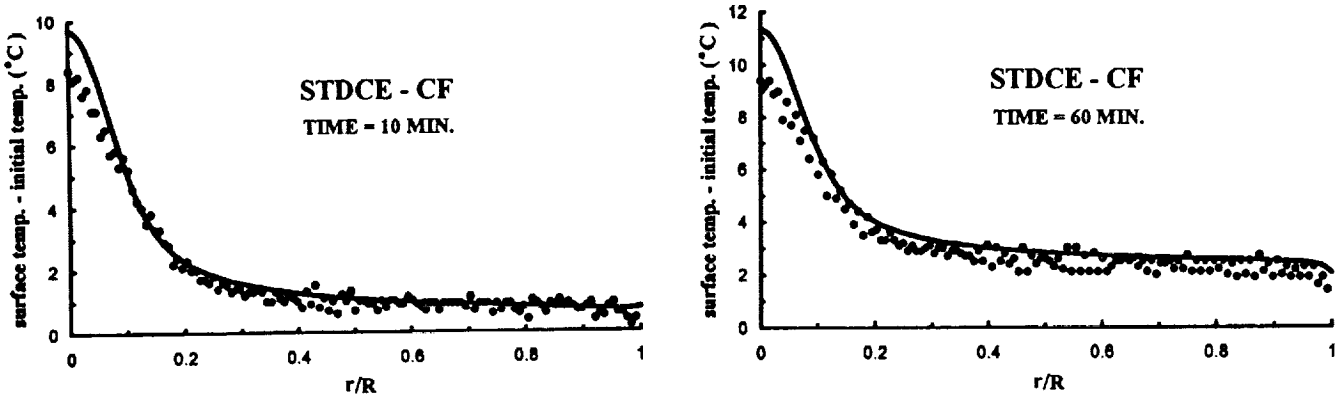

Figure 18 Comparison of infrared imager data with numerical result for CF test

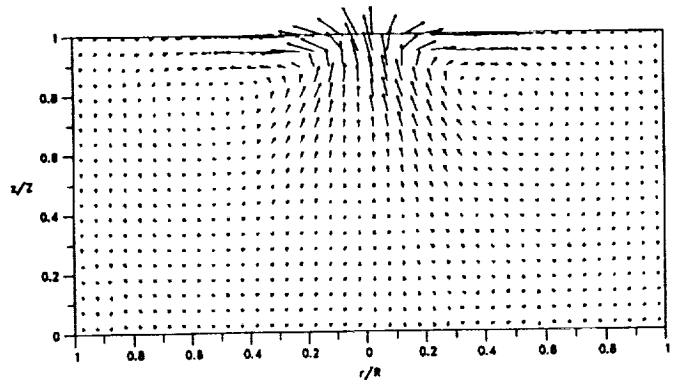

Figure 19 Measured velocity vectors at t = 10 min. for CF test

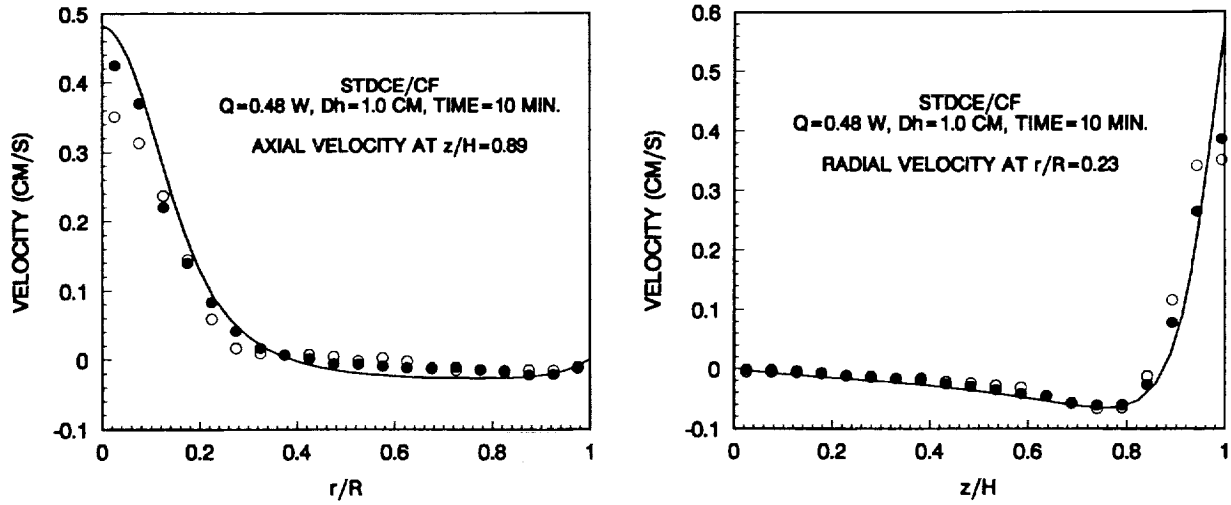

Figure 20 Measured and computed velocity distributions at t = 10 min. for CF test

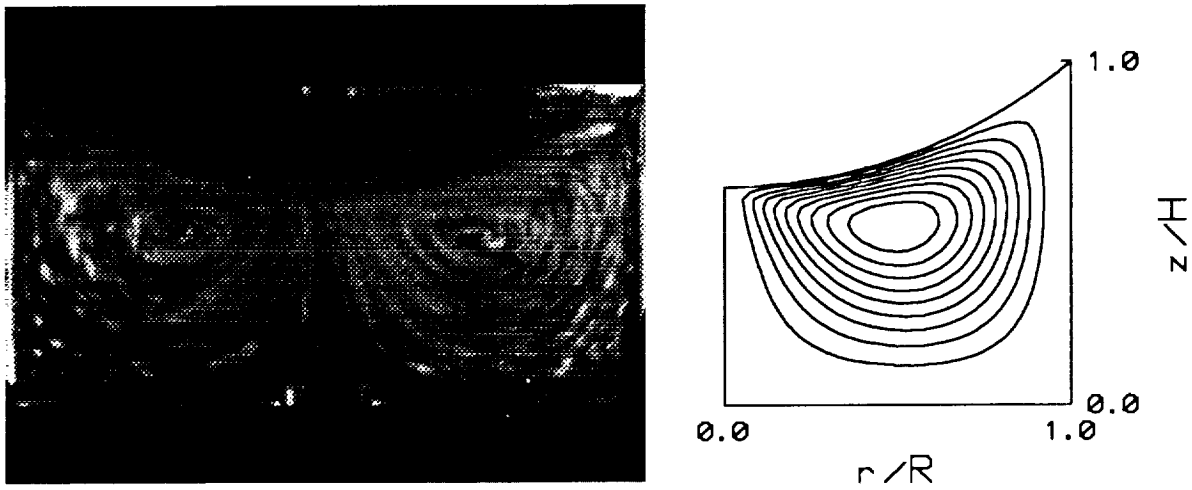

(a) Observed streamlines

(b) Computed streamlines

Figure 21 Observed and computed streamlines for a curved free surface test in CF configuration (Q = 1.4 W, beam dia. = 5 mm)

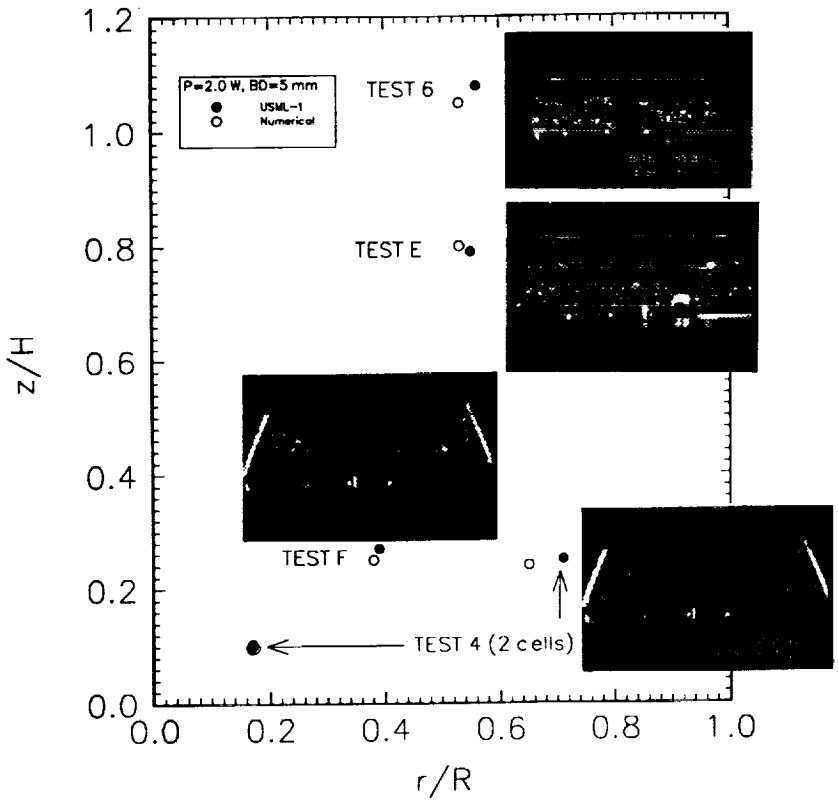

Figure 22 Experimental and numerical comparison of cell center locations for CF tests

Discussion

Question: *Could you make a comment as to what you think is wrong in terms of the prediction for oscillatory onset that does not seem to happen. Where do you think the problem is ?*

Answer: Well, the problem is in the physics. You know there was just always this assumption that was an instability. Usually if you think of an instability you can see a physical mechanism for an instability, that you have a heavy fluid overlaying a lighter one. When the thing (oscillatory behavior in surface tension flows) was called an instability, I did not see that physics. We went along with it and it became apparent to us that we could not correlate the onset conditions with a single parameter. The only other, if you believe in similitude theory which I do, I am a strong advocate of it, you say there is another parameter missing. Well what is the other parameter ? From the boundary conditions and the normal stresses there is a capillary number. Now everybody was taught to evaluate the capillary number. The capillary number, if you evaluate it, is very small. So you say that surface deformation cannot be important. We had a heated discussion about this here in Huntsville in the early days before any experiments were done. There had been some numerical studies where people had assumed a linear temperature profile along the free surface and I as an applied mathematician said, the surface temperature distribution has to be part of the solution. We got into this argument, and also considered the shape, and people said that since the capillary numbers are very small, it was not important. But when we could not correlate the data, we knew we needed another parameter, and asked the question what can that be ? The answer is the capillary number, which immediately said surface deformation must be important and so we said that. As we continue to do experimental and numerical work we feel, and we have described this, that the oscillations are due to a three way coupling, part of the inherent dynamics of the situation. In other words, you impose a temperature gradient on the free surface, when the Marangoni number gets effectively high so the convection is important, that is why you have got to exceed the Marangoni number like 10^4. What happens is that profile begins to change and the imposed signature changes. For high Prandtl number fluids it actually becomes S-shaped so that all the driving ends up in the end. Now this fluid moves to the end, hits the end wall and because the surface can deform, even if it deforms a little bit, there is a time lag. So the return flow that comes back and starts to cool has that time lag in it. You say this S parameter, which is a modified capillary number, is kind of small but that S parameter is a measure of the deformation of the free surface to the radius. Well that is a very small number but the fact is that the thermal boundary layer thicknesses here are 100 microns. So these deformations are on that order. So what is happening is that the driving force is being modulated through this time lag. And now everybody in the world sees these deformations of the free surface. Our feeling is that it is not an instability. All the instability theories have to date left off the end

effects, they have dealt with doubly infinite regimes and they claim quantitative agreement. They will agree with a wave number but be off 3 orders of magnitude on the frequency. The wave forms are wrong and so this has been some sort of a controversy that has been going on. At the same time I hear people saying we understand the physics of Marangoni convection. Maybe the physics of Marangoni flow they understand but thermocapillary flows, the physics, has been a problem. And I think we have gone a long way to delineate it. And I think unequivocally, our measurements have shown the importance of the ends in driving this whole mechanism.

Question: *Was it the stream function maximum that you compared from the experiment to the calculations?*
Answer: Yes.

Question: *In your numerical code how did you input the shape of the surface ? Was that calculated or was that a constant? And did you get that from the experiment ?*
Answer: Knowing the contact angle the shape is determined and input to the code.

Question: *What are your reasons for the marginal, at best, comparisons ? I did not understand why your numerical prediction of the circulation center point did not agree with the experiment ?*
Answer: Because these rotating cells, these sub-region flows which occur in buoyancy driven flows as well, have velocities that are sometimes orders of magnitude off the mean velocity. So if your computer doesn't know where these cells are and what high resolution to use, they miss it just like experimentally you would miss it if you didn't have the right resolution. That has been the problem in trying to do confined flows by buoyancy driven or by surface tension driven force where the driving is being done on the surface. What happens in the interior can be all kind of crazy things like what I call flow sub-regions. If you don't have the proper resolution numerically or experimentally you are going to miss those and that is the problem.

Question: *That means it is not a converged solution. It has to be grid independent. Is that correct ?*
Answer: True. That is an inherent difficulty. People think all you have to do is compute everything. When I have people computing 3 dimensional, unsteady, turbulent everything I give them a little problem of a box, heat one wall and then cool one wall. I'll show you what the data looks like. I never hear from those guys again. So it is not that easy.